

# Universal programmable metasurface building blocks for arbitrary high-order mode conversion

JINLONG XIANG<sup>†</sup>, ZHIYUAN TAO<sup>†</sup>, XUHAN GUO<sup>\*</sup>, YONG ZHANG, YAOTIAN ZHAO, AND YIKAI SU

*State Key Laboratory of Advanced Optical Communication Systems and Networks Department of Electronic Engineering, Shanghai Jiao Tong University, Shanghai 200240, China*

*<sup>†</sup> These authors contributed equally to this work.*

*<sup>\*</sup>Corresponding author: guoxuhan@sjtu.edu.cn*

**Abstract:** On-chip integrated mode-division multiplexing (MDM) has been emerging as a promising technology to further improve the link capacity and satisfy the continuously increasing bandwidth demand in data communications. One of the most important components in MDM and multimode photonics is a mode converter. While several configurations have been developed to realize on-chip mode converters, it is still very challenging to achieve versatile high-order mode converters with high performance in a generic way to reduce the R&D and prototyping costs. Here we initiate a breakthrough utilizing a simple yet universal generic building block concept with metasurface structures to implement programmable arbitrary high-order mode converters with competitive performance, high reliability and compact footprints. The building block, i.e., the TE<sub>0</sub>-TE<sub>2</sub> mode converter is first introduced to illustrate the generic concept, which exhibits low insertion loss of 0.3 dB, low crosstalk of -10 dB across broad wavelength band of 250 nm with a footprint of  $2.7 \times 1.3 \mu\text{m}^2$ . All even-order and odd-order mode converters can be realized by directly programming multiple parallel basic building blocks and coarsely engineering the waveguide widths simply in a universal approach. The proposed mode converter building blocks for high-order mode conversion highlight features of uniform performance with broad bandwidth, low insertion loss, compact footprints and good fabrication tolerance, plus the uniquely simple and scalable generic fashion, making them extremely attractive for on-chip multimode optical interconnections.

## 1. Introduction

Advanced multiplexing technologies have been playing extremely important roles to satisfy the continuously increasing demands for high capacity of data communication [1-4]. MDM technology, which leverages the extra degree of freedom of orthogonal guiding modes in multimode waveguides, is emerging to boost significantly the scalability and flexibility of the transmission capacity [5, 6]. Benefiting from its compact footprint and compatibility with the complementary metal-oxide-semiconductor (CMOS) fabrication process, silicon on-chip MDM system has attracted extensive attention. Various MDM devices have been demonstrated on a silicon-on-insulator (SOI) platform, such as mode (de)multiplexers [7-15], mode exchangers [16, 17], mode filters [18, 19], mode switches [20-22], multimode crossings [23, 24], multimode waveguide bends [25, 26] and reconfigurable multimode photonic devices [15, 16, 27]. Among them, mode converters which can transform given modes into desired modes are the fundamental and integral devices to build a practical MDM system.

Previously, significant efforts have been devoted to realize efficient on-chip mode conversions. The working principles of these devices can be generally categorized into the following four types [28]. (i) Phase matching method: The basic idea is to choose the appropriate waveguide width to guarantee that the mode in the access waveguide has the same effective refractive index with the desired mode in the bus waveguide. Considerable mode converters and mode (de)multiplexers implemented with asymmetry directional couplers (ADCs) have been reported [8, 9, 13, 29] based on this principle. To further improve the

fabrication tolerance thus scaling up the mode channel numbers, subwavelength grating structures (SWG) have been proposed [30-32]. Besides, there are other resonant coupling devices including both directional grating couplers and contra-directional grating assisted couplers [33-35]. (ii) Constructive interference of coherent scattering: The input mode will evolve into various high-order modes which interfere with each other in the conversion region. Consequently, the desired mode profile can be formed at the output port. Traditionally, multimode interference (MMI) couplers [36-38], photonic crystal waveguides [39, 40] or cascaded tapers [41] are employed. Moreover, several computer-generated nanostructures based on inverse-design algorithms have also been demonstrated [42-45]. (iii) Beam forming technique: The concept follows that the  $N_n$  ( $N \geq 1$ ) order TE mode can be treated as a combination of  $N+1$  antiphase adjacent  $TE_0$ -like modes. To obtain the  $TE_n$ - $TE_0$  mode converter, the  $N+1$  antiphase components of the  $TE_n$  mode should travel through different effective lengths in the conversion field, thus achieving the same phase and eventually to combine into the  $TE_0$  mode. Typically, Mach-Zehnder interferometer (MZI) structures are utilized, given that the phase differences between their arms can be flexibly tuned [16, 46, 47]. (iv) Metasurface: Recently, quite a few mode converters based on metasurface structures have been proposed for both the TE polarization [48-55] and the TM polarization [56, 57]. The mode conversion between two specific modes is achieved by imposing specific refractive-index perturbations on a silicon waveguide.

An ideal mode converter should have the merits of mode conversion with low insertion loss (IL), low crosstalk, broad bandwidth, compact footprints, and large fabrication tolerance. On-chip mode multiplexing systems, where particular modes are allocated to optimally perform desired functionalities, however, require considerable designs and optimization iterations of different mode conversion structures leading to long development times [28]. It should be noticed that for method (i), the different high-order modes inevitably incur different designs to satisfy the phase matching conditions, and it will become almost impossible for both ADC and SWG structures to be extended for modes order higher than 15 ( $N > 15$ ) mode converters, owing to the large effective refractive index contrast between two concerned modes. Arbitrary high-order mode converters, in principle, can be obtained with the last three strategies, but all with compromised performance. (ii-iii) usually come with large footprints. Although ultra-compact mode converters have been reported with decent performance utilizing the inverse design methodology, its computation time will drastically increase when scaled up to higher-order mode ( $N > 3$ ). Meanwhile, the irregular nanostructures normally demand fabrication techniques with high accuracy, making it less feasible in real applications. (iv) represents the most compact devices reported by far, but higher-order mode converters ( $N > 5$ ) haven't been experimentally demonstrated. Therefore, a simple solution to unlimited high-order mode converters with constant good performance, compact footprints, high scalability and feasibility in practice for multimode multiplexing photonics is extremely desirable.

In this paper, we propose for the first time, to the best of our knowledge, a universal scheme to program arbitrary high-order mode converters in an easy yet generic building block approach. This method is inspired by electronic Field Programmable Gate Arrays (FPGA), where any arbitrary high-order mode converters can be implemented by a simple topology consisting of basic low-order mode converters to realize different multimode functionalities through programming. We first introduce our design philosophy with the primitive  $TE_0$ - $TE_2$  mode converter exploiting fully etched dielectric metasurface slots in the SOI platform, which will function as the basic building block for high-order mode converters. The simulated insertion loss is less than 0.3 dB and the crosstalk is lower than -10 dB across the wavelength band from 1400 nm to 1650 nm. The operating principles are theoretically analyzed using the beam shaping technique together with the coupled mode theory (CMT). After that, any even-order mode converters can be acquired by simply programming parallel arrangement of a set of  $TE_0$ - $TE_2$  mode converters with an appropriate waveguide width. Employing the same approach, any odd-order mode converters can be realized by directly shifting and cutting off part of the even-

order mode converters with a fixed width. We emphasize that the performance of all the programmed arbitrary ultra-high-order mode converters can still maintain impressively well with the insertion loss less than 1.5 dB as well as crosstalk lower than -9 dB over an ultra-broad bandwidth of 250 nm.

## 2. Design philosophy and building block

Previously we have reported an ultra-compact mode-order converter by exploiting a fully etched silica slot on a silicon waveguide, which can efficiently serve as both a power splitter and a phase shifter at the same time [55]. Now we further develop this concept for universal mode conversions, utilizing the metasurface structures to realize the straightforward beam forming technique. We impose fully etched dielectric perturbations on silicon waveguides to split the input fundamental mode into  $N+1$  beams with nearly equal power and simultaneously induce a  $\pi$  phase difference between contiguous components. As a result, the  $N_{th}$ -order mode can be successfully formed at the end of the perturbations within several micrometers. In the following section, we take the  $TE_0$ - $TE_2$  mode converter as an example to illustrate the design methodology in detail and provide the theoretical analysis with the CMT model.

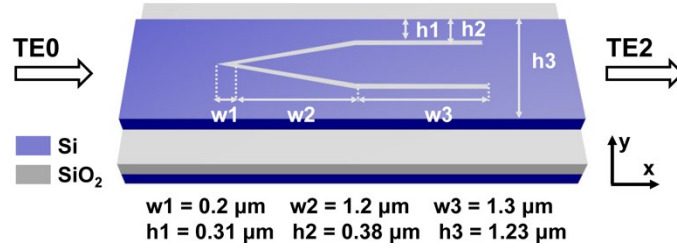


Fig. 1. Schematic of the  $TE_0$ - $TE_2$  mode converter.

In the basic  $TE_0$ - $TE_2$  mode converter building block, the perturbation in the metasurface structure is initialized with a symmetric polygon shape as shown in Fig. 1. The two straight arms separate the multimode waveguide into three single-mode waveguides, where three  $TE_0$ -like components will transmit through. We sweep the variables in 3D finite-difference-time-domain (FDTD) simulations and the optimized parameters are given in Fig. 1. Figure 2(a) presents the simulated electric field distribution at the wavelength of 1550 nm, which clearly shows the  $TE_0$ - $TE_2$  mode conversion. The simulated transmission spectrum is given in Fig. 2(b). The insertion loss is less than 0.3 dB, while the crosstalk is lower than -10 dB from 1400 nm to 1650 nm. The curve ‘other’ stands for the total crosstalk from other modes except for the  $TE_0$  mode and the  $TE_2$  mode.

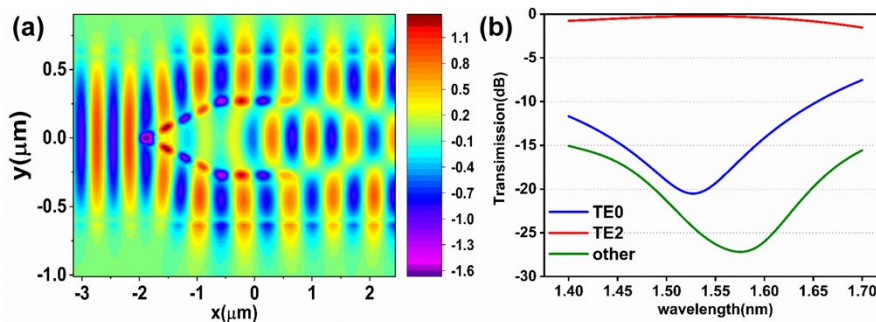


Fig. 2. Simulated electric field distribution (a) and transmission spectra (b) of the  $TE_0$ - $TE_2$  mode converter

The evolution of optical field in a perturbed structure can be described by the CMT model (see the theoretical analysis in Section 1, supporting information). Figure 3(a) presents the mode purity from both numerical calculations of CMT model (curves) and FDTD simulation

(symbols) along the propagation direction, which agree quite well with each other. It's clear that the input  $TE_0$  mode is gradually converted into the  $TE_2$  mode within a short length less than  $3\ \mu\text{m}$ . Fig. 3(b) shows the coupling coefficients as a function of the propagation distance, which is not sinusoidal-like owing to the aperiodic perturbations. It's necessary for  $\kappa_{02}$  to change from positive to negative value, ensuring that the  $TE_0$  mode always contributes constructively to the conversion of the  $TE_2$  mode. Fortunately, there is almost zero crosstalk from the  $TE_1$  mode due to the negligible  $\kappa_{01}$ .

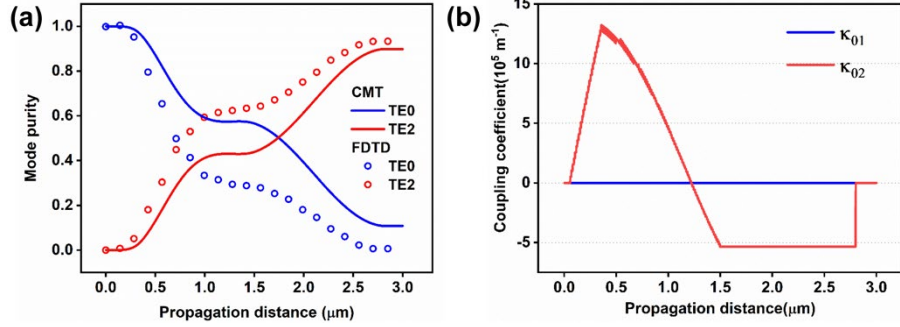


Figure 3. Mode evolution (a) and coupling coefficients (b) as a function of propagation distance.

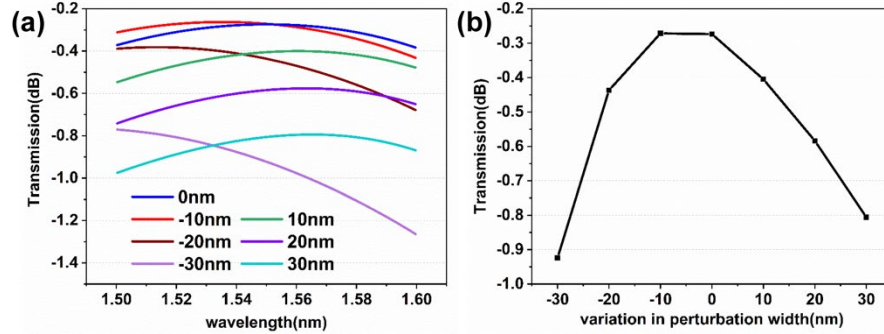


Fig. 4. Transmission spectra (a) and the insertion loss at 1550 nm (b) of the  $TE_0$ - $TE_2$  mode converter with different perturbation width.

To further extend for arbitrary high-order mode converters, it's essential that the basic building block should be insensitive to the fabrication imperfections. We analyze the fabrication tolerance of the  $TE_0$ - $TE_2$  mode converter by evaluating the mode conversion efficiency influenced by the random deviation for the perturbation width. As shown in Fig. 4, the insertion loss keeps lower than 1 dB across the whole 100 nm bandwidth even though the variation reaches up to  $\pm 20\text{nm}$ . Undoubtedly, the robustness of the basic building block guarantees the stable performance of the high-order mode converters.

### 3. Implementation of arbitrary high-order mode converters

#### 3.1 Even-order mode converters

We now demonstrate that all even-order mode converters can be obtained by simply programming the same parallel perturbations with the  $TE_0$ - $TE_2$  mode converter building blocks. Although an individual building block can generate three channels, the two light beams on both sides actually have the same phase. To satisfy the anti-phase relation between neighboring beams, the distance between two adjacent building blocks has to be narrowed to generate only one channel. Consequently, total  $2M+1$  channels can be generated by  $M$  building blocks. Therefore,  $N/2$  building blocks are needed to design a  $N_{th}$ -order ( $N$  is an even number) mode converter, and the waveguide width can be expressed by

$$W_{\text{even}} = d \cdot \frac{N}{2} + 2W_{\text{extra}} (\mu\text{m}) \quad (1)$$

where  $d$  is the central distance between adjacent building blocks, and  $w_{\text{extra}}$  is the applied extra waveguide width to better confine the guided modes. The optimized parameters from FDTD simulations are  $d = 0.92 \mu\text{m}$  and  $W_{\text{extra}} = 0.19 \mu\text{m}$ , respectively.

As an example, the structure of the  $\text{TE}_0$ - $\text{TE}_6$  mode converter is presented in Fig. 5. Three same  $\text{TE}_0$ - $\text{TE}_2$  mode converters are programmed in a parallel array, and the whole structure is vertical symmetric along the propagation direction. Only seven  $\text{TE}_0$ -like channels are formed in the conversion region due to the narrow gaps between two adjacent building blocks. As depicted in Fig. 6 (a), total seven beams are progressively generated and eventually combine into the expected  $\text{TE}_6$  mode. Figure 6 (b) presents the simulated conversion efficiency and modal crosstalk. The insertion loss is measured to be less than 1 dB and the crosstalk is below -9.5 dB from 1400 nm to 1700 nm. Besides, the major crosstalk comes from the  $\text{TE}_4$  mode.

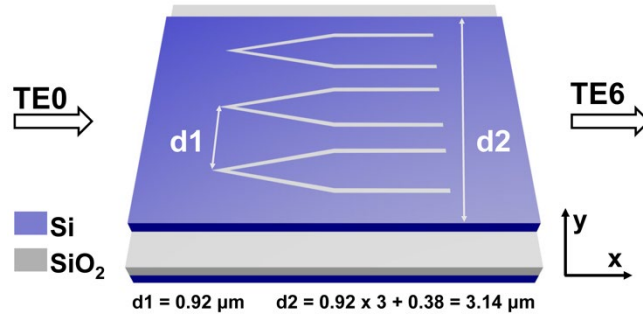


Fig. 5. Schematic of the  $\text{TE}_0$ - $\text{TE}_6$  mode converter.

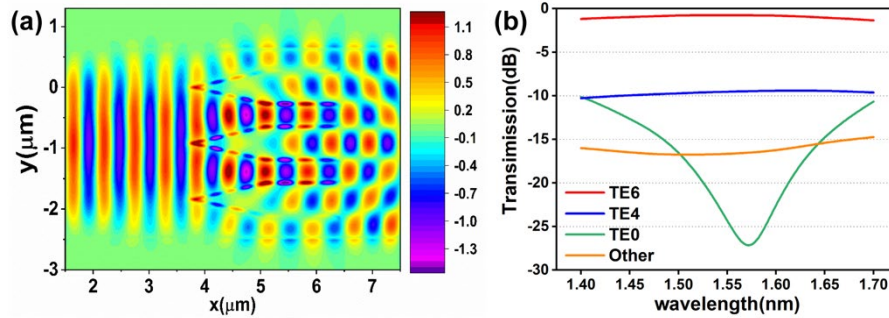


Fig. 6. Simulated electric field distribution (a) and conversion efficiency (b) of the  $\text{TE}_0$ - $\text{TE}_6$  mode converter.

Actually, this approach can be extended for any even-order mode converters by programming the proper numbers of parallel building block and waveguide widths as discussed above. As a proof of concept, we simulate an unprecedented high-order  $\text{TE}_0$ - $\text{TE}_{28}$  mode converter. As presented in Fig. 7, twenty-nine  $\text{TE}_0$ -like modes with anti-phase between adjacent beams are finally formed at the end of the perturbations. Besides, the insertion loss is still less than 1.5 dB and the modal crosstalk maintains lower than -9 dB from 1400 nm to 1650 nm. It's worth noting that the crosstalk mainly results from the neighboring guided mode  $\text{TE}_{26}$ , due to the similarity between their mode profiles. Although this is undesired and unavoidable, it may provide us with another simpler way to test the coupling efficiency of the ultra-high-order mode converters. Instead of quantifying the crosstalk from each single mode in traditional methods, we only focus on the specific modes causing the major crosstalk.

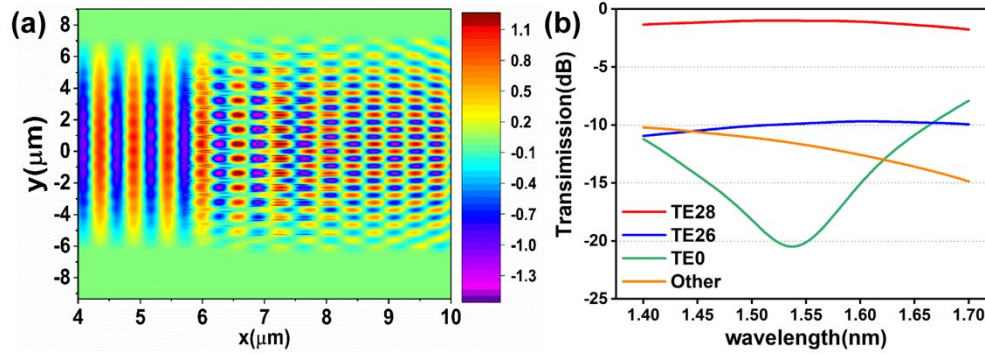


Fig. 7. Simulated electric field distribution (a) and conversion efficiency (b) of the TE<sub>0</sub>-TE<sub>28</sub> mode converter.

### 3.2 Odd-order mode converters

To further extend the generality of the proposed generic building block concept, we demonstrate the implementation of arbitrary high odd-order mode converters on the basis of even-order mode converters. To design a  $N_m$ -order ( $N$  is an odd number) mode converter, we reduce one waveguide channel of the TE<sub>0</sub>-TE<sub>n+1</sub> mode converter by directly cutting off part of the structure on one side with a fixed width, which is much smaller than the original waveguide width. Fortunately, the evolution of optical field will just be slightly influenced, thus remaining the desired  $N$  single-mode channels. (This method is not suitable for the TE<sub>1</sub> and TE<sub>3</sub> mode, and their implementations based on the same design concept are given in Section 2, supporting information). Furthermore, the waveguide width for odd-order mode converters can be expressed by

$$W_{odd} = d \cdot \frac{N+1}{2} + 2W_{extra} - W_{cutoff} \quad (\mu m) \quad (2)$$

where  $W_{cutoff}$  is the width of the truncated part, and the optimized value is  $0.46 \mu m$ .

As an example, the schematic diagram of the TE<sub>0</sub>-TE<sub>5</sub> mode converter is shown in Fig. 8, which is exactly the same as that of the TE<sub>0</sub>-TE<sub>6</sub> mode converter, except  $0.46 \mu m$  wide structure is cut off on the upper side. The simulated electric field distribution and the transmission curves are given in Fig. 9 (a) and Fig. 9 (b) respectively. The insertion loss is less than 1 dB and the crosstalk is below -10 dB with a large bandwidth of 300 nm. Likewise, we give the simulation results for the ultra-high TE<sub>0</sub>-TE<sub>27</sub> mode converters to show the scalability. The TE<sub>27</sub> mode consisting of twenty-eight TE<sub>0</sub>-like beams can be obviously observed in Fig. 10 (a). Moreover, the insertion loss keeps less than 1.5 dB and the crosstalk still maintains lower than -9 dB from 1400 nm to 1650 nm. Similarly, as shown in the figure, the TE<sub>25</sub> mode accounts for the major crosstalk.

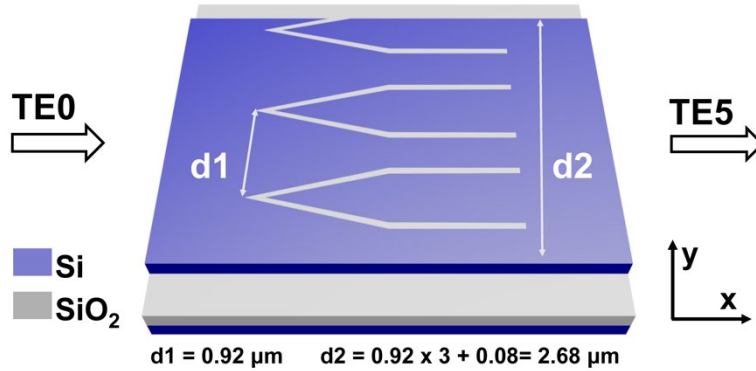


Fig. 8. Schematic of the TE<sub>0</sub>-TE<sub>5</sub> mode converter.

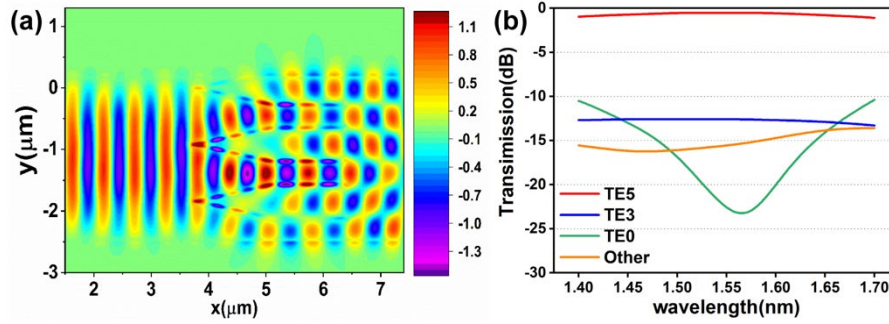


Fig. 9. Simulated electric field distribution (a) and conversion efficiency (b) of the  $TE_0$ - $TE_5$  mode converter

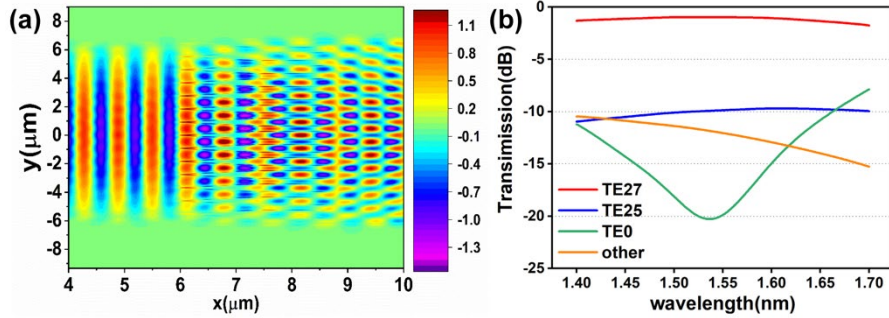


Fig. 10. Simulated electric field distribution (a) and conversion efficiency (b) of the  $TE_0$ - $TE_{27}$  mode converter

#### 4. Discussion and Conclusion

We now give a summary of the universal design for arbitrary high-order mode converters based on the programmed metasurface building blocks in Figure 11. We provide both the overall layouts and the important design parameters. We also give the estimated performance of the programmed building-block-implemented arbitrary mode converters: the insertion loss is predicted to be approximately 1.5 dB. Besides, the neighboring  $TE_{n-2}$  mode is the major source of the modal crosstalk, which is estimated to be nearly -9 dB within a broad bandwidth from 1400 nm to 1650 nm. Finally, the device is tolerant to the fabrication errors up to  $\pm 20$  nm variation in the perturbation width.

We emphasize that the footprint of the proposed mode converter increases linearly with the mode order, promising high integration intensity. Since we just engineer the building blocks in a generic rough way, the acquired decent performance can be further improved by coarse-tune the parameters (e.g., the waveguide width, the distance between building blocks) for specific mode converters. Moreover, the mode coupling efficiency can be flexibly tailored by adjusting the arm lengths of the building blocks as presented in Fig. 3.

It is worth noting that the proposed mode converters can function as mode exchangers at the same time, which can be hardly realized by most traditional mode converters. (see the analysis of mode exchangers in Section S3, supporting information) Although a universal approach to realize mode exchangers has been reported [17], the design is mode-specific and need to be re-optimized repeatedly. Besides, the involved parameter space will grow rapidly as the increase of concerned mode order. In contrast, the presented devices can be conveniently obtained by program the building blocks appropriately, and no extra optimization complexity is needed.

More importantly, the proposed programmable building block concept can be efficiently migrated to other platforms (e.g., InP,  $Si_3N_4$ , etc.) as well as other wavelength-bands (e.g., mid-infrared band, etc.), which will definitely open the opportunity to better control the multimode

light on-chip. The manipulation of multiple modes simultaneously will not only increase the link capacity in optical communication systems, but also potentially find applications in quantum information processing [58], nonlinear photonics [59], photonic sensing [60], etc.

In conclusion, by employing the programmable compact metasurface building blocks, we report a universal methodology to realize the mode conversion between the fundamental mode and arbitrary high-order mode for the first time. All the even-order and odd-order mode converter can be efficiently realized by programming the parallel array of the building block, i.e., the TE<sub>0</sub>-TE<sub>2</sub> mode converter and coarsely control the waveguide widths. The proposed devices feature constant performance of broad bandwidth (from 1400 nm to 1650 nm), low insertion loss (<1.5 dB), low modal crosstalk (-9 dB), compact footprints and robustness to the fabrication variations (up to ±20 nm). This will give significant inspirations to other device designs and could promise a great breakthrough to boost the development of on-chip MDM systems

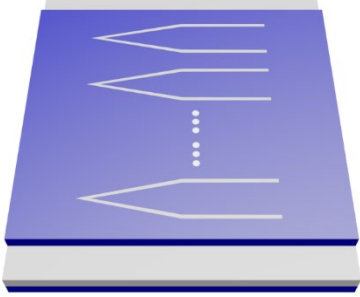

Programmable arbitrary mode converters	Parameters	Performance (Est.)
 <p data-bbox="386 1119 630 1186"><b>Even-order mode converters</b></p>	<p data-bbox="776 842 1027 873"><math>N/2</math> building blocks</p> <hr/> <p data-bbox="776 1077 1027 1108"><b>Waveguide width:</b></p> $W_{\text{even}} = d \cdot \frac{N}{2} + 2W_{\text{extra}} (\mu\text{m})$	<p data-bbox="1138 905 1268 1010"><b>Insertion loss:</b> ~1 dB</p> <p data-bbox="1138 1052 1268 1157"><b>Major crosstalk:</b> TE<sub>N-2</sub></p> <p data-bbox="1138 1199 1268 1304"><b>Modal crosstalk:</b> ~10dB</p>
 <p data-bbox="386 1623 630 1690"><b>Odd-order mode converters</b></p>	<p data-bbox="756 1325 1047 1392"><math>(N+1)/2</math> building blocks with edge truncation</p> <hr/> <p data-bbox="776 1577 1027 1608"><b>Waveguide width:</b></p> $W_{\text{odd}} = d \cdot \frac{N+1}{2} + 2W_{\text{extra}} - W_{\text{cutoff}} (\mu\text{m})$	<p data-bbox="1122 1346 1284 1451"><b>Bandwidth:</b> 1500-1600nm</p> <p data-bbox="1122 1493 1284 1598"><b>Fabrication tolerance:</b> ±30 nm</p>

Fig. 11. Universal design of the  $N_{th}$ -order mode converter.



**Funding.** National Key R&D Program of China (2019YFB2203101); Natural Science Foundation of China (NSFC) (61805137 and 61835008); Natural Science Foundation of Shanghai (19ZR1475400); Shanghai Sailing Program (18YF1411900); Open Project Program of Wuhan National Laboratory for Optoelectronics (2018WNLOKF012).

**Disclosures.** The authors declare no conflicts of interest.

## References

1. R. Soref, "Mid-infrared photonics in silicon and germanium," *Nature photonics* **4**, 495 (2010).
2. K. Wada, H.-C. Luan, D. R. Lim, and L. C. Kimerling, "On-chip interconnection beyond semiconductor roadmap: Silicon microphotonics," in *Active and Passive Optical Components for WDM Communications II*, (International Society for Optics and Photonics, 2002), 437-443.
3. R. Soref, "The past, present, and future of silicon photonics," *IEEE Journal of selected topics in quantum electronics* **12**, 1678-1687 (2006).
4. B. Jalali and S. Fathpour, "Silicon photonics," *Journal of lightwave technology* **24**, 4600-4615 (2006).
5. P. J. Winzer, "Making spatial multiplexing a reality," *Nature Photonics* **8**, 345 (2014).
6. D. Richardson, J. Fini, and L. E. Nelson, "Space-division multiplexing in optical fibres," *Nature Photonics* **7**, 354 (2013).
7. Y. Li, C. Li, C. Li, B. Cheng, and C. Xue, "Compact two-mode (de) multiplexer based on symmetric Y-junction and multimode interference waveguides," *Optics express* **22**, 5781-5786 (2014).
8. D. Dai, J. Wang, S. Chen, S. Wang, and S. He, "Monolithically integrated 64-channel silicon hybrid demultiplexer enabling simultaneous wavelength- and mode-division-multiplexing," *Laser & Photonics Reviews* **9**, 339-344 (2015).
9. J. Wang, S. He, and D. Dai, "On-chip silicon 8-channel hybrid (de)multiplexer enabling simultaneous mode- and polarization-division-multiplexing," *Laser & Photonics Reviews* **8**, L18-L22 (2014).
10. L. Han, S. Liang, H. Zhu, L. Qiao, J. Xu, and W. Wang, "Two-mode de/multiplexer based on multimode interference couplers with a tilted joint as phase shifter," *Opt. Lett.* **40**, 518-521 (2015).
11. D. González-Andrade, J. G. Wangüemert-Pérez, A. V. Velasco, A. Ortega-Moñux, A. Herrero-Bermello, I. Molina-Fernández, R. Halir, and P. Cheben, "Ultra-broadband mode converter and multiplexer based on sub-wavelength structures," *IEEE Photonics Journal* **10**, 1-10 (2018).
12. K. Mehrabi and A. Zarifkar, "Ultracompact and broadband asymmetric directional-coupler-based mode division (de) multiplexer," *JOSA B* **36**, 1907-1913 (2019).
13. L.-W. Luo, N. Ophir, C. P. Chen, L. H. Gabrielli, C. B. Poitras, K. Bergmen, and M. Lipson, "WDM-compatible mode-division multiplexing on a silicon chip," *Nature communications* **5**, 3069 (2014).
14. Daoxin, Dai, Chenlei, Li, Shipeng, Wang, Hao, Wu, Yaocheng, and Shi, "10-Channel Mode (de)multiplexer with Dual Polarizations," *Laser & Photonics Reviews* (2017).
15. H. Xiao, Z. Liu, H. Xu, J. Yang, G. Ren, M. Arnan, and Y. Tian, "On-chip reconfigurable and scalable optical mode multiplexer/demultiplexer based on three-waveguide-coupling structure," *Optics Express* **26**, 22366- (2018).
16. C. Sun, Y. Yu, G. Chen, and X. Zhang, "Integrated switchable mode exchange for reconfigurable mode-multiplexing optical networks," *Opt. Lett.* **41**, 3257-3260 (2016).
17. J. Guo, C. Ye, C. Liu, M. Zhang, C. Li, J. Li, Y. Shi, and D. Dai, "Ultra-Compact and Ultra-Broadband Guided-Mode Exchangers on Silicon," *Laser & Photonics Reviews* **n/a**, 2000058 (2020).
18. W. Jiang, J. Miao, T. Li, and L. Ma, "Low-loss and broadband silicon mode filter using cascaded plasmonic BSWGs for on-chip mode division multiplexing," *Optics Express* **27**, 30429-30440 (2019).
19. Y. HE, Y. ZHANG, H. WANG, and Y. SU, "On-chip silicon mode blocking filter employing subwavelength-grating based contra-directional coupler," *Optics Express* **26**, 33005 (2018).
20. Y. Xiong, R. B. Priti, and O. Liboiron-Ladouceur, "High-speed two-mode switch for mode-division multiplexing optical networks," *Optica* **4**, 1098-1102 (2017).
21. J. Lv, T. Lian, B. Lin, Y. Yang, Y. Cao, X. Yang, Y. Yi, F. Wang, and D. Zhang, "Low Power Consumption Mode Switch Based on Three-Dimensional Polymer Mach-Zehnder Interferometer," *IEEE Photonics Journal* **12**, 1-10 (2020).
22. S. Zheng, X. Cao, and J. Wang, "Multimode Fano resonances for low-power mode switching," *Opt. Lett.* **45**, 1035-1038 (2020).
23. H. Xu and Y. Shi, "Ultra - Sharp Multi - Mode Waveguide Bending Assisted with Metamaterial - Based Mode Converters," *Laser & Photonics Reviews* **12**, 1700240 (2018).
24. W. Chang, L. Lu, X. Ren, L. Lu, M. Cheng, D. Liu, and M. Zhang, "An ultracompact multimode waveguide crossing based on subwavelength asymmetric Y-junction," *IEEE Photonics Journal* **10**, 1-8 (2018).
25. X. Jiang, H. Wu, and D. Dai, "Low-loss and low-crosstalk multimode waveguide bend on silicon," *Optics express* **26**, 17680-17689 (2018).
26. Y. Wang and D. Dai, "Multimode silicon photonic waveguide corner-bend," *Optics Express* **28**, 9062-9071 (2020).

27. R. Tang, T. Tanemura, S. Ghosh, K. Suzuki, K. Tanizawa, K. Ikeda, H. Kawashima, and Y. Nakano, "Reconfigurable all-optical on-chip MIMO three-mode demultiplexing based on multi-plane light conversion," *Opt. Lett.* **43**, 1798-1801 (2018).
28. Y. Su, Y. Zhang, C. Qiu, X. Guo, and L. Sun, "Silicon Photonic Platform for Passive Waveguide Devices: Materials, Fabrication, and Applications," *Advanced Materials Technologies* **n/a**, 1901153 (2020).
29. D. Dai, J. Wang, and Y. Shi, "Silicon mode (de)multiplexer enabling high capacity photonic networks-on-chip with a single-wavelength-carrier light," *Opt. Lett.* **38**, 1422-1424 (2013).
30. Y. He, Y. Zhang, H. Wang, L. Sun, and Y. Su, "Design and experimental demonstration of a silicon multi-dimensional (de)multiplexer for wavelength-, mode- and polarization-division (de)multiplexing," *Opt. Lett.* **45**, 2846-2849 (2020).
31. Y. He, Y. Zhang, Q. Zhu, S. An, R. Cao, X. Guo, C. Qiu, and Y. Su, "Silicon high-order mode (De) multiplexer on single polarization," *Journal of Lightwave Technology* **36**, 5746-5753 (2018).
32. W. Jiang and X. Wang, "Ultra-Broadband Mode Splitter Based on Phase Controlling of Bridged Subwavelength Grating," *Journal of Lightwave Technology* **38**, 2414-2422 (2020).
33. Ming-Chan, Wu, Fu-Chen, Hsiao, Shuo-Yen, and Tseng, "Adiabatic Mode Conversion in Multimode Waveguides Using Chirped Computer-Generated Planar Holograms," *Photonics Technology Letters IEEE* (2011).
34. S. Y. Tseng and M. C. Wu, "Adiabatic Mode Conversion in Multimode Waveguides Using Computer-Generated Planar Holograms," *IEEE Photonics Technology Letters* **22**, 1211-1213 (2010).
35. H. Qiu, H. Yu, T. Hu, G. Jiang, H. Shao, P. Yu, J. Yang, and X. Jiang, "Silicon mode multi/demultiplexer based on multimode grating-assisted couplers," *Optics Express* **21**, 17904 (2013).
36. H. D. T. Linh, T. C. Dung, K. Tanizawa, D. D. Thang, and N. T. Hung, "Arbitrary  $\text{TE}_0/\text{TE}_1/\text{TE}_2/\text{TE}_3$  Mode Converter Using  $1 \times 4$  Y-Junction and  $4 \times 4$  MMI Couplers," *IEEE Journal of Selected Topics in Quantum Electronics* **PP**, 1-1 (2019).
37. J. Leuthold, J. Eckner, E. Gamper, P. A. Besse, and H. Melchior, "Multimode interference couplers for the conversion and combining of zero- and first-order modes," *Journal of Lightwave Technology* **16**, 1228-1239 (1998).
38. D. Gonzalez-Andrade, J. G. Wanguemert-Perez, A. Velasco, A. Ortega-Monux, A. Herrero-Bermello, I. Molina-Fernandez, R. Halir, and P. Cheben, "Ultra-broadband mode converter and multiplexer based on sub-wavelength structures," *IEEE Photonics Journal*, 1-1 (2018).
39. V. Liu, D. A. B. Miller, and S. Fan, "Ultra-compact photonic crystal waveguide spatial mode converter and its connection to the optical diode effect," *Optics Express* **20**, 28388 (2012).
40. Gang, Chen, Jin, and Kang, "Waveguide mode converter based on two-dimensional photonic crystals," *Opt. Lett.* (2005).
41. D. Chen, X. Xiao, L. Wang, Y. Yu, W. Liu, and Q. Yang, "Low-loss and fabrication tolerant silicon mode-order converters based on novel compact tapers," *Optics express* **23**, 11152-11159 (2015).
42. H. Xie, Y. Liu, S. Wang, Y. Wang, Y. Yao, Q. Song, J. Du, Z. He, and K. Xu, "Highly Compact and Efficient Four-Mode Multiplexer Based on Pixelated Waveguides," *IEEE Photonics Technology Letters* **32**, 166-169 (2020).
43. H. Jia, H. Chen, T. Wang, H. Xiao, G. Ren, A. Mitchell, J. Yang, and Y. Tian, "Multi-channel Parallel Silicon Mode-order Converter for Multimode On-chip Optical Switching," *IEEE Journal of Selected Topics in Quantum Electronics* (2019).
44. H. Ma, J. Huang, K. Zhang, and J. Yang, "Ultra-compact and efficient  $1 \times 2$  mode converters based on rotatable direct-binary-search algorithm," *Optics Express* **28**, 17010-17019 (2020).
45. H. Jia, H. Chen, J. Yang, H. Xiao, W. Chen, and Y. Tian, "Ultra-compact dual-polarization silicon mode-order converter," *Opt. Lett.* **44**, 4179-4182 (2019).
46. B.-T. Lee and S.-Y. Shin, "Mode-order converter in a multimode waveguide," *Opt. Lett.* **28**, 1660-1662 (2003).
47. Y. Huang, G. Xu, and S.-T. Ho, "An Ultracompact Optical Mode Order Converter," *IEEE Photonics Technology Letters* **18**, p.2281-2283 (2006).
48. H. Wang, Y. Zhang, Y. He, Q. Zhu, L. Sun, and Y. Su, "Compact Silicon Waveguide Mode Converter Employing Dielectric Metasurface Structure," *Advanced Optical Materials* **7**, 1801191 (2018).
49. Zhaoyi, Li, Myoung-Hwan, Kim, Cheng, Wang, Zhaohong, Han, Sajan, and Shrestha, "Controlling propagation and coupling of waveguide modes using phase-gradient metasurfaces," *Nature Nanotechnology* (2017).
50. D. Ohana, B. Desiatov, N. Mazurski, and U. Levy, "Dielectric Metasurface as a Platform for Spatial Mode Conversion in Nanoscale Waveguides," *Nano Letters* **16**, 7956-7961 (2016).
51. L. Hao, R. Xiao, Y. Shi, P. Dai, Y. Zhao, S. Liu, J. Lu, and X. Chen, "Efficient TE-Polarized Mode-Order Converter Based on High-Index-Contrast Polygonal Slot in a Silicon-on-Insulator Waveguide," *IEEE Photonics Journal* **11**, 1-10 (2019).
52. B. E. Abu-Elmaaty, M. S. Sayed, R. K. Pokharel, and H. M. Shalaby, "General silicon-on-insulator higher-order mode converter based on substrip dielectric waveguides," *Appl. Opt.* **58**, 1763-1771 (2019).
53. D. Ohana and U. Levy, "Mode conversion based on dielectric metamaterial in silicon," *Optics express* **22**, 27617-27631 (2014).

54. Z. Cheng, J. Wang, Z. Yang, L. Zhu, Y. Yang, Y. Huang, and X. Ren, "Sub-wavelength grating assisted mode order converter on the SOI substrate," *Optics Express* **27**, 34434-34441 (2019).
55. Y. Zhao, X. Guo, K. Wang, H. Wang, and Y. Su, "Ultra-Compact Silicon TE-Polarized Mode Converters Combining a Directional Coupler and a Phase Shifter," in *Asia Communications and Photonics Conference*, (Optical Society of America, 2019), M3D. 4.
56. L. Liu, Y. Xu, L. Wen, Y. Dong, B. Zhang, and Y. Ni, "Design of a compact silicon-based TM-polarized mode-order converter based on shallowly etched structures," *Appl. Opt.* **58**, 9075-9081 (2019).
57. Y. Xu, C. Zhu, X. Hu, Y. Dong, B. Zhang, and Y. Ni, "On-chip silicon shallowly etched TM<sub>0</sub>-to-TM<sub>1</sub> mode-order converter with high conversion efficiency and low modal crosstalk," *Journal of the Optical Society of America B* **37**, 1290-1297 (2020).
58. A. Mohanty, M. Zhang, A. Dutt, S. Ramelow, P. Nussenzveig, and M. Lipson, "Quantum interference between transverse spatial waveguide modes," *Nature Communications* **8**, 14010 (2017).
59. E. A. Kittlaus, N. T. Otterstrom, and P. T. Rakich, "On-chip inter-modal Brillouin scattering," *Nature Communications* **8**, 15819 (2017).
60. N. Hoppe, T. Fohn, P. Diersing, P. Scheck, and M. Berroth, "Design of an Integrated Dual-Mode Interferometer on 250 nm Silicon-on-Insulator," *IEEE Journal of Selected Topics in Quantum Electronics* **PP**, 1-1 (2016).